A comparative study of the structure of hydro-products derived from Loblolly Pine and Straw Grass

Qiong Wu [a]*, Lang Huang [b], Shitao Yu [a], Shiwei Liu [a], Congxia Xie [a] and Arthur J. Ragauskas [c d]*

[a]*College of Chemical Engineering, Qingdao University of Science and Technology, 53 Zhengzhou Road, Qingdao, Shandong province 266042, PR China*

[b]*Composite Material and Engineering Center, Washington State University, PACCAR Rm 112, 2001 East Grimes Way, Pullman, WA, USA, 99164*

[c]*Department of Chemical & Biomolecular Engineering, University of Tennessee Knoxville, 419 Doughterty Engineering Bldg, Knoxville, TN, USA, 37996*

[d]*Joint Institute of Biological Science, Biosciences Division, Oak Ridge National Laboratory, Oak Ridge, TN, USA,37830*

* Corresponding author: College of Chemical Engineering, Qingdao University of Science and Technology, 53 Zhengzhou Road, Qingdao, Shandong province 266042, PR China

Tel: +86 53284022719 E-mail: wuqiong0506@hotmail.com (Q Wu)

Abstract

The structural characteristics of products derived from the hydrothermal carbonization (HTC) of Loblolly Pine (LP) and Straw Grass (SG) were investigated via Solid-State Cross-Polarization/Magic Angle Spinning nuclear magnetic resonance (CP/MAS ^{13}C NMR), Heteronuclear Single-Quantum Correlation Nuclear Magnetic Resonance (HSQC-NMR), solution ^{13}C NMR and ^{31}P NMR techniques. Results revealed that after HTC, hydrochars from both LP and SG mainly consisted of a combination of lignin, furfural and condensed polyaromatic structures with a high level of fixed carbon content and Higher Heating Value (HHV). Hydrochar from the LP exhibited a higher aryl to furan ratio, and those from the SG contained more aliphatic functional groups. Solution ^{13}C NMR and HSQC revealed that both liquid chemicals were condensed polyphenolic structures with aliphatic groups, that existing mainly in the form of side chains. Although the LP products exhibited a higher proportion of aromatic structures, the types of polyphenol and aliphatic C-H were more diverse in the SG products. Results also indicated that reactions such as chain scission and condensation occurred during the hydrothermal carbonization processes. Overall, HTC was found to be an effective refinery treatment for converting different waste biomass into valuable energy materials and chemicals.

Keywords: Biomass; Thermal conversion; Carbonaceous materials; NMR techniques

Introduction

Lignocellulose substances such as grass, poplar, pine and corn are the most

abundant and readily utilized biomass resources in the world. They all have the potential to be converted into value-added products used in the fields of adsorption, catalysis and energy.[1-3] Although they have the same basic components, the percentages of these components vary greatly. For example pine mainly consist of ~46% cellulose, lignin percentage account for the second (~28%) with hemicellulose percentage is the third (~23%). However, in grass-related materials, content of hemicellulose reached to 26~33%, and lignin account for only 17~18%.[4] The obvious differences among the composition of raw materials can lead to structural and character differences in the final chemicals they are used to produce, including the ratio of aromatic structures, oxygen-containing functional groups and species of intermediate products created during the conversion process.[5]

Similar to the process of "coaling", hydrothermal carbonization (HTC) is an effective method for converting biomass materials into carbon materials and other valuable energy chemicals.[6] Bergius[7] first described the transformation of cellulose into coal-like materials in 1913. Since then, the HTC process has been rapidly developed for the production of various carbonaceous materials. HTC involves reactions conducted in a closed system under mild temperatures (120-280 °C) using water and self-generated pressure. The resulting materials are a black solid powder and a sticky liquid. The solid product has been reported to have abundant functional groups such as carbonyl, carboxyl and hydroxyl which can be used in environmental and energy fields as catalysts,[8] adsorbents,[9] super-capacitors[10] and electrode materials[11] while liquid products can be further treated yielding fuels, chemicals and/or materials.[12]

So far, literature about the hydrothermal treatment of complex biomass has

provided a limited and inconsistent picture of the products' chemical composition and reaction paths, and few comparative studies have been conducted. The solid products of HTC such as hydrochar have been characterized using FT-IR, Raman spectroscopy, X-ray photoelectron spectroscopy (XPS) and X-ray diffraction (XRD) techniques using polysaccharides as raw materials,[13,14] while liquid products have not been studied as much. The amorphous character, chemical complexity and heterogeneity of HTC products challenge most analytical characterization techniques. FT-IR and XPS spectroscopy techniques do not have enough resolution to precisely depict the structure of HTC products, as the spectra are poorly resolved and composed of several overlapping peaks. Xiao et al.[15] has used Gas Chromatography-Mass Spectrometer (GC-MS) to analyze HTC liquid products and was shown to be an effective means to identify selective products, but the product mixture is complex and has many overlapping peaks that cannot be determined. Compared to these techniques, NMR has a much higher resolution and can provide detailed structural information on both solid and liquid hydrothermal products. This technique can provide qualitative or semi-quantitative data for structure identification of organic compounds based on chemical shift data.[16] Our previous works examined the chemical structure of hydro-products using CP/MAS ^{13}C NMR and quantitative ^{13}C NMR, and it proved that NMR techniques can provide an accurate chemical-shift assignment database for a corresponding structural analysis.[17,18] On this basis, Heteronuclear Single-Quantum Correlation-Nuclear Magnetic Resonance (HSQC-NMR)—which is a 2D spectrum that can provide a directly connected relationship between hydrogen and carbon for

the intuitive and accurate judgment of structures[19]—will be applied. In this study, we focused on a comparative study of the structure of hydrochars and liquid-chemicals, choosing two different kinds of biomass—LP and SG—as raw materials, and using combination of 1D and 2D NMR techniques.

Based on some of our previous investigations, we propose here that 240 ^{o}C is the appropriate temperature and 4 h is the appropriate time period for converting lignocellulose resources into carbon materials in our laboratory.[20] These conditions are based on yields and structure and energy consumption; therefore, for this present research, we conducted all of our experiments at 240 ^{o}C and 4 h. The goal of this work is to provide a guide for the utilization of different kinds of biomass based on demand for solid/liquid structure components.

Experimental

Materials

LP woodchips and SG were collected from a Kraft pulp mill in the Georgia, United States. The air-dried materials were milled to around 0.50 mm, then Soxhlet-extracted with methylene chloride for 24 h, and stored in a desiccator for further use.

HTC Experimental procedure

10.00 g of dried LP and SG powders (moisture content 6.25%, dry weight of 9.38 g) were dispersed in 150 ml of distilled water and ultrasonically agitated for 15 min at room temperature (RT). The mixtures were then transferred to a 200 ml Parr pressure reactor (Parr Instrument Company, Moline, Illinois), and the reactor was heated to 240 ^{o}C and held at this temperature for 4 h. The reaction mixtures were then

allowed to cool to RT and centrifuged to separate the liquid phase from the solid products. The black solid products were further washed with DI water until the effluent was clear and then dried in a vacuum at 80 °C overnight and labeled as CSP_{240}-4 (from the LP) and CSG_{240}-4 (from the SG). The liquid products were stored in a freezer for further use after being freeze dried.

Characterization

Raw Materials and Hydrochar (Solid products)

Klason lignin content analysis: the original LP, SG and corresponding hydrochar samples was acid hydrolyzed with a two-step acid hydrolysis according to previous published literature.[21] The acid insoluble residues known as Klason lignin were filtered through a G8 glass fiber filter (Fisher Scientific, USA), dried, and weighed.

Solid-State Cross-Polarization/Magic Angle Spinning nuclear magnetic resonance (CP/MAS ^{13}C NMR) spectra were recorded at RT using a Bruker Avance III 400 spectrometer (Bruker Biospin AG, Fallanden) operating at a frequency of 100.55 MHz for ^{13}C in a Bruker double-resonance MAS preheated at spinning speeds of 10 kHz. CP/MAS experiments utilized a 5 μs (90 ^{o}) proton pulse, a 2.0 ms contact pulse, a 4 s recycle delay and 8000 scans. NMR data processing and plots were carried out using the MestReNova v7.1.0 software's default processing template (zero-filling is 32 K) with a line-broadening (LB) of 5.0 Hz and automatic phase and baseline correction.

The weight average molecular weight (Mw), number average molecular weight (Mn) and polydispersity index (Eqs.1) of the original LP, SG, CSP_{240}-4 and CSG_{240}-4

were determined by Gel Permeation Chromatography (GPC) analysis using methods from the relevant existing literature.[22]

$$PDI=Mw/Mn \quad (1)$$

Prior to GPC analysis, the acetylation solid samples were dissolved in THF (1 mg/mL), which exhibited good solubility and was filtered through a 0.45 μm syringe filter prior to analysis.

Ash content was tested using a Pyris1 TGA apparatus (Perkin Elmer, USA) at a heating rate of 20 °C min^{-1} in air.

The HHV was expressed on a dry basis, and evaluated using the Dulong's formula (Eqs.2) and measured in an adiabatic oxygen bomb calorimeter according to the TAPPI method T684 om-06 (TAPPI Test Methods, 2006).

$$HHV = 0.3383 \times C + 1.422 \times (H-O/8) \quad (2)$$

Liquid products

All liquid NMR spectrum data in this study were recorded with a Bruker Avance/DMX 400 MHz NMR spectrometer. All the NMR data processing and plots were carried out using the MestReNova v7.1.0 software's default processing template (zero-filling is 32 K) with a line-broadening (LB) of 5.0 Hz and automatic phase and baseline correction.

Quantitative ^{13}C-NMR acquisition was employed with the following acquisition parameters: ~100.0 mg liquid products dissolved in 450 μL DMSO-d_6; ^{13}C-NMR acquisition was performed on a QNP probe operating at a frequencies of 100.59 MHz, using a 90° pulse with an inverse-gated decoupling pulse sequence, a 12-s pulse delay,

and 12288 scans at RT; the central DMSO solvent peak was used for calibrating chemical shifts.

A standard Bruker Heteronuclear Single-Quantum Correlation Nuclear Magnetic Resonance (HSQC) was used on a BBO probe with the following acquisition parameters: spectra width 10 ppm in F2 (^{1}H) dimension with 2048 times of domain (acquisition time 256.1 ms); 210 ppm in F1 (^{13}C) dimension with 256 times of domain (acquisition time 6.1 ms), a 1.5-s delay, and 32 scans. The central DMSO solvent peak ((C/ (H at 39.5/2.49) was used for calibrating chemical shifts.

Quantitative ^{31}P NMR were acquired after *in situ* derivatization of the samples using ~20 mg of samples with 2-chloro-4,4,5,5-tetramethyl-1,3,2-dioxaphospholane (TMDP) in a solution of (1.6:1 v/v) pyridine/$CDCl_3$, chromium acetylacetonate (relaxation agent), and Endo-N-hydroxy-5-norbornene-2,3-dicarboximide (NHND, internal standard). Quantitative ^{31}P NMR spectra were acquired on a Bruker Advance 400 MHz spectrometer equipped with a BBO probe using an inverse-gated decoupling pulse sequence (Waltz-16), a 90° pulse, and a 25-spulse delay with 64 scans and a total runtime of 28 min. All chemical shifts reported are relative to the product of TMDP with water, which was observed to provide a sharp signal in the pyridine/$CDCl_3$ at 132.2 ppm. The contents of the hydroxyl groups were quantitated on the basis of the amount of added internal standard.

Results and Discussion

Chemical and structure properties of LP, SG and hydrochars

The hydrochar yield, fixed carbon content, ash content and HHV of LP, SG,

CSP_{240}-4 and CSG_{240}-4 were summarized and are shown in Table 1. The main components of the LP and SG were the same, while there were obvious differences in the percentages of each component.[4] The LP consisted mainly of 39.88% glucan, 32.06% klason lignin and 18.63% hemicellulosic sugars; while the SG consisted of 37.94% glucan, 25.37% hemicellulosic sugars, and only 24.91% klason lignin, while its ash content was higher (not shown). After HTC treatment, the hydrochars showed a remarkable change in their compositional components, as compared with the original LP and SG. In the hydrochars, the klason lignin content reached 97.52 % for CSP_{240}-4 and 94.67% for CSG_{240}-4, indicating that the final hydrochars consisted mainly of condensed lignin-like components,--in fact, a combination of lignin and polyphenolic structures—generally referred to as pseudo lignin, as our group has studied in details previously.[23]

SG typically contains a higher content of cellulose and hemicellulose, which are unstable and can be hydrolyzed easily; therefore, in our experiment, we found that its solid yield was only 41.93%, lower than the 45.50% of CSP_{240}-4. Both exhibited a high fixed carbon content—48.61% (CSG_{240}-4) and 53.16% (CSP_{240}-4)—confirming that HTC is an effective means for carbon sequestration. The fixed carbon content of the CSG_{240}-4 was lower for two reasons; first, the fixed carbon content of the SG itself was lower and second, the percentage of unstable components such as ash in the SG was higher. The HHV of the CSG_{240}-4 and CSP_{240}-4 also exhibited significant differences: the value for CSG_{240}-4 was 23.94 MJ/kg, nearly 1.48 times that of the untreated SG. Comparable to many other HTC materials,[24,25] this value for the

CSP_{240}-4 reached as high as 29.34 MJ/kg, which was even higher than that of the coal reported in some of the literature.[26] The results shown in Table 1 also indirectly indicate that there were still abundant components stored in the liquid products, especially for the CSG_{240}-4.

Table 1

CP/MAS ^{13}C NMR was used to characterize the detailed differences among the chemical structures of the LP, SG and corresponding hydrochars, as shown in Fig. 1 and Table S1. The spectrum can be divided into three spectral domains: between 0 and 100 ppm, indicating the presence of aliphatic and ether carbons; between 100 and 160 ppm, with carbon atoms in C=C double bonds; and at 160-250 ppm, for which signals represent C=O groups in either carboxylic acid moieties or ketones and aldehydes.[27-28] From Fig. 1, it is clear that after HTC, a large amount of unsaturated aromatic structures were formed in both hydrochars, and indeed, aromatic structures became the main structures in the hydrochars. There were also abundant aliphatic functional groups generated, especially in the CSG_{240}-4, which derived from the higher content of cellulose and hemicellulose in the SG.

The detailed chemical shifts assignments are shown in Table S1. The peaks in the range of 119-142 ppm arose from the condensed aromatic structures, pointing out that the final hydrochars belonged to the poly-aromatic structure. The signals centered at 151 ppm, corresponding with the O–C=C groups in the aromatics as well as with the C_a in the furan units.[29] Signals in the range of 106 and 117 ppm arose from the C=C-R groups, indicating the existence of furfuran structures within the poly-

aromatic structures, as reported in the literature.[30] Aliphatic alkanes and methyl carbons were also generated, as indicated by the signals centered at 30-37 ppm and 23 ppm, which were more abundant in the CSG_{240}-4. It may be concluded that the structural components of the two hydrochars were similar but with different proportions. The CSP_{240}-4 contained a higher percentage of aromatic structures, and the peak intensity centered at 117 ppm was much lower than that centered at 151 ppm, indicating that the ratio of furan to arene was less than one, and the aromatic structure was still the primary structure.[31] In the CSG_{240}-4, the ratio of furan to arene was still less than one, but the ratio value was higher than that of the CSP_{240}-4. This suggests that a higher proportion of furan was generated in the CSG_{240}-4 than in the CSP_{240}-4, as furan mainly forms via the hydrolysis products of cellulose and hemicellulose, which were more abundant in the SG.

Fig.1

The number average, weight average molecular weights (Mn and Mw) and polydispersity index (PDI) values of the CSP_{240}-4 and CSG_{240}-4 are shown in Fig. 2: they all display the same change trend with the values of Mw having decreased and the Mn having increased slightly after HTC treatment. This reveals a general shift of the high molecular weight fraction to the lower molecular weight, indicating that chain scission occurred. At the same time, the PDI values exhibited the same trend, showing that their molecular weight distributions were narrower.

Fig. 2

Composition of Hydrothermal liquid products

Solution ^{13}C NMR was used for further quantitative analysis of the functional groups of the CSP_{240}-4 and CSG_{240}-4 liquid chemicals, and the integration results are summarized in Fig. 3. Overall, the CSP_{240}-4 and CSG_{240}-4 were rich in aromatic carbon, including aromatic C-C, C-O and C-H bonds, suggesting that polyaromatic groups were the main structure. The newly generated aromatic C-O and C-C bonds mainly derived from radical-initiated condensation reactions between aromatic and aliphatic hydroxyl groups,[32,33] as well from the polymerization and substitution reactions. Aliphatic C-O and C-C bonds were also abundant, especially in the CSG_{240}-4, showing that the liquid products also consisted of polyphenolic and aliphatic alkane groups. For liquid products, the CSP_{240}-4 was still more rich in condensed aromatic structures, while the CSG_{240}-4 contained more aliphatic chain groups; in contrast, more groups containing C=O were detected in the liquid than in the solid products for both.

Fig. 3

HSQC provides a facile way to elucidate the component structures (C-H connection methods) in the liquid hydro-products. The assignments of furfural, aromatic C-H bonds, aliphatic C-H bonds and methoxyl groups in the HSQC-NMR spectra for the liquid products of the CSP_{240}-4 and CSG_{240}-4 are shown in Figures 5-8, separately. The corresponding detailed structures of the assignments are listed in Fig. 4 and based on previous studies.[34-39] The results confirmed completely that the furans and polyphenols with alkanes are major structures that exist in liquid products, in accordance with our analysis above.

Fig. 4

Fig. 5 confirms the existence of furfural structures. A represents the C-H bond of the aldehyde group in the furfural, and B represents the C-H bond of hydroxymethyl in the furans. The CSG_{240}-4 contained both C-H bonds in furfural and an HMF structure, while only the furfural structure was detected in the CSP_{240}-4. The aromatic C-H bonds indicated that the major aromatic components in the CSG_{240}-4 were liquid products containing C, D, E, F, G, H and I types of aromatic C-H bonds as shown in Fig. 6, while only C, D, E, F, G types existed in the CSP_{240}-4. From ^{13}C NMR analysis, we can see that the CSP_{240}-4 was more abundant in aromatic C-C bonds, which may suggest that the aromatic structure of the CSP_{240}-4 was more condensed. Fig. 7 indicates that the CSG_{240}-4 was more abundant in aliphatic C-H bonds of both contents and types. The M, N and J types of aliphatic C-H bonds were the main form for both products, pointing out that aliphatic groups existed mainly in the form of aromatic side chains. Fig. 8 shows that methoxyl existed mainly in two forms, and these were more often to be rearranged methoxyl (O_1, no hydroxyl group or ether bond in the ortho position) than O_2 for both products.

The results indicate that although the CSP_{240}-4 contained more condensed polyphenol structures (detected via ^{13}C NMR), the types of phenols and aliphatic C-H were more diverse in the CSG_{240}-4.

Fig. 5

Fig. 6

Fig. 7

Fig. 8

^{31}P NMR was used to quantitatively analyze the special hydroxyls groups in the liquid products. The contrast ^{31}P NMR figures of the CSP_{240}-4 and CSG_{240}-4 are shown in Fig. 9, and the assignment ranges and corresponding structures have been referenced in the literature[40] as shown in Table 2. The peaks between 145-150 ppm are aliphatic hydroxyls that were more obvious and rich for the CSG_{240}-4, while the peaks between 137.5-140.2 ppm are free phenolic hydroxyls, which were richer for the CSP_{240}-4. Peaks appearing around 134 ppm are mostly carboxylic acid OH. Consistent with the results produced via NMR characterization, we found that the CSP_{240}-4 experienced more aromatization, while the CSP_{240}-4 was more abundant with aliphatic groups.

Fig. 9

Per the detailed contents shown in Table 2, a greater amount of non-condensed phenolic units than C_5 substituted phenolic units were observed for both products. The total hydroxyl content of liquid products was 5.73 mmol/g for the CSP_{240}-4 and 6.97 mmol/g for the CSG_{240}-4, and the condensed hydroxyl content was 0.27 mmol/g and 0.07 mmol/g, respectively.

Free phenolic hydroxyls in liquid products came primarily from catechol and guaiacyl units, and it is believed that at the initial stage, the thermal cleavage of the β-O-4 ether bond will form guaiacyl, a p-hydroxy-phenyl hydroxyl group, and catechols; this has been studied by Ben et al.[41] who found that mostly monomeric phenols were generated. Carboxylic acids OH were abundant, which occurred mostly toward the

end of the aromatic side-chain.

Table 2

Conclusion

Through hydrolysis, chain scission, polymerization, aromatization and condensation reactions that occurred during HTC, the LP and SG were effectively converted into condensed carbon materials with high HHV (hydrochar) and water-soluble chemicals; the materials produced consisted mainly of polyphenolic compounds and furan derivatives that are desirable feedstock for biodiesel and chemical production. The hydrochar of the CSP_{240}-4 exhibited a more condensed polyaromatic structure, with a fixed carbon content of 53.16%. The HHV was as high as 29.34 MJ/kg, nearly 1.46 times that of the LP. A high aryl to furan ratio was exhibited, and the degree of aromatization was higher than that of the CSG_{240}-4. The CSG_{240}-4 contained more aliphatic and carboxyl groups, and had a fixed carbon value of 48.61% and an HHV value as high as 23.94 MJ/kg, nearly 1.48 times that of the SG. Liquid products for both were condensed polyphenolic structures with aliphatic side chains, although in the liquid products, the CSP_{240}-4 exhibited more aromatization, the types of polyphenol, and the furan and aliphatic groups, were richer and diverse in the CSG_{240}-4.

In conclusion, the hydrochar obtained from LP exhibited higher fixed carbon content, HHV and degree of aromatization, which are more suitable used as carbon materials to replace fossil carbon sources, while SG are more appropriate feedstocks for liquid chemicals production such as biodiesel and platform chemicals.

Supporting Information

CP/MAS ^{13}C NMR chemical shift assignment ranges and functional group contributions

Acknowledgements

This work was financially supported by the Taishan Scholars Program of Shandong Province (ts201511033).

The authors declare no competing financial interest.

Reference

1 Zhao, L.; Fan, L. Z.; Zhou, M. Q.; Guan, H.; Qiao, S. Y.; Antonietti, M. Nitrogen-containing hydrothermal carbons with superior performance in supercapacitors. *Adv. Mater.* **2010**, *22*, 5202-5206.

2 Wu, Q.; Li, W.; Tan, J.; Liu, S. X. Hydrothermal carbonization of carboxymethylcellulose: One-pot preparation of conductive carbon microspheres

and water-soluble fluorescent carbon nanodots. *Chem. Eng. J.* **2015**, *266*, 112-120.

3 Reza, M. T.; Yang, X. K.; Coronella, C. J.; Lin, H. F.; Hathwaik, U. Hydrothermal carbonization (HTC) and pelletization of two arid land plants bagasse for energy densification. *ACS Sustain. Chem. Eng.* **2016**, *4*, 1106-1114.

4 Ragauskas, A. J.; Beckham, G.T.; Biddy, M.J.; Chandra, R.; Chen, F.; Davis, M. F. Lignin Valorization: Improving Lignin Processing in the Biorefinery. *Science.* **2014**, *344*, 1246843-1-1246843-10.

5 Titirici, M. M.; Antonietti, M.; Baccile. N. Hydrothermal carbon from biomass: a comparison of the local structure from poly- to monosaccharides and pentoses/hexoses. *Green Chem.* **2008**, *10*, 1204-1212.

6 Titirici, M. M.; Thomas, A.; Yu, S. H.; Antonietti, M. A direct synthesis of mesoporous carbons with bicontinuous pore morphology from crude plant material by hydrothermal carbonization. *New J. Chem.* **2007**, *31*, 787-789.

7 Bergius, F. Die Anwendung hoher Drucke bei chemischen Vorga¨ngen und eine Nachbildung des Entstehungsprozesses der Steinkohle, Verlag Wilhelm Knapp, Halle an der Saale. *Germany* **1913**.

8 Sun, R. Q.; Sun, L. B.; Chun,Y.; Xu, Q. H. Catalytic performance of porous carbons obtained by chemical activation. *Carbon*, **2008**, *46*, 1757-1764.

9 Xue, Y. W.; Gao, B.; Yao, Y.; Inyang, M. D.; Zhang, M.; Zimmerman, A. R.; Ro, K. S. Hidrogen peroxide modification enhances the ability of biochar (hydrochar) produced from hydrothermal carbonization of peanut hull to remove aqueous heavy metals: Batch and column tests *Chem. Eng. J.* **2012**, *15*, 673-680.

10 Zhao, L.; Fan, L. Z.; Zhou, M. Q.; Guan, H.; Qiao, S. Y.; Antonietti, M.; Titirici, M. M. Nitrogen-Containing Hydrothermal Carbons with Superior Performance

in supercapacitors. *Adv. Mater.* **2010**, *22*, 5202-5206.

11 Huggins, T.; Wang, H. M.; Kearns, J.; Jenkins, P.; Ren, Z. Y. J. Biochar as a sustainable electrode material for electricity production in microbial fuel cells. *Bioresour. Technol.* **2014**, *157*, 114-119.

12 Sun, H. Q.; Zhou, G. L.; Wang, Y. X.; Suvorova, A.; Wang, S. B. A new metal-free carbon hybrid for enhanced photocatalysis. *ACS Appl. Mater. Inter.* **2014**, *6*, 16745-16754.

13 Sun, X. M.; Li, Y. D. Colloidal carbon spheres and their core/shell structures with noble-metal nanoparticles. *Angew. Chem. Int. Ed.* **2004**, *43*, 597-601.

14 Sevilla, M.; Fuertes, A. B. The production of carbon materials by hydrothermal carbonization of cellulose. *Carbon*, **2009**, *47*, 2281-2289.

15 Xiao, L. P.; Shi, Z. J.; Xu, F.; Sun, R. C. Hydrothermal carbonization of lignocellulosic biomass. *Bioresour. Technol.* **2012**, *118*, 619-623.

16 Foston, M.; Nunnery, G. A.; Meng, X. Z.; Sun, Q. N.; Baker, F. S.; Ragauskas, A. J. NMR a critical tool to study the production of carbon fiber from lignin. *Carbon* **2013**, *52*, 65-73.

17 Foston, M.; Nunnery, G. A.; Meng, X. Z.; Sun, Q. N.; Baker, F. S.; Ragauskas, A. J. NMR a critical tool to study the production of carbon fiber from lignin. *Carbon* **2013**, *52*, 65-73.

18 Wu, Q.; Li, W.; Tan, J.; Liu. S. X. Flexible cage-like carbon spheres with ordered mesoporous structures prepared via a soft-template/hydrothermal process from carboxymethylcellulose. *RSC Adv.* **2014**, *4*, 61518-61524.

19 Yoo, C. G.; Pu, Y. Q.; Li, M.; Ragauskas. A. J. Solution-state 2D NMR with a mixture of deuterated dimethylsulfoxide and hexamethylphosphoramide. *Chemsuschem* **2016**, *9*, 1090-1095.

20 Wu, Q.; Li, W.; Wu, P.; Li, J.; Liu, S. X.; Jin C. D. Effect of reaction temperature on properties of carbon nanodots and their visible-light photocatalytic degradation of tetracycline. *RSC Adv.* **2015**, *5*, 75711-75721.

21 Hu, Z.; Sykes, R.; Davis, M. F.; Charles, B. E.; Ragauskas, A. J. Chemical profiles of switchgrass. *Bioresour. Technol.* **2010**, *101*, 3253-3257.

22 Ben, H.; Ragauskas, A. J. NMR Characterization of Pyrolysis Oils from Kraft Lignin. *Energy Fuels* **2011**, *25*, 2322-2332.

23 Hu, F.; Jung, S.; Ragauska, A. Pseudo-lignin formation and its impact on enzymatic hydrolysis. *Bioresource Technol.* **2012**, *117*, 7-12.

24 Mumme, J.; Eckervogt, L.; Pielert, J.; Diakitem, M.; Rupp, F.; Kern, J. Hydrothermal carbonization of anaerobically digested maize siage. *Bioresource Technol.* **2011**, *102*, 9255-9260.

25 Hoekman, S. K.; Broch, A.; Robbins, C. Hydrothermal carbonization (HTC) of lignocellulosic biomass. *Energy Fuels* **2011**, *25*, 1802-1810.

26 Channiwala, S. A.; Parikh, P. P. A unified correlation for estimating HHV of solid, liquid and gaseous fuels. *Fuel* **2002**, *81*, 1051-1063.

27 Melkior, T.; Jacob, S.; Gerbaud, G.; Hediger, S.; Pape, L. L.; Bonnefois, L. NMR analysis of the transformation of wood constituents by torrefaction. *Fuel* **2012**, *92*, 271-280.

28 Neupane, S.; Adhikari, S.; Wang, Z.; Ragauskas, A. J.; Pu, Y. Q. Effect of torrefaction on biomass structure and hydrocarbon production from fast pyrolysis. *Green Chem.* **2015**, *17*, 2406-2417.

29 Falco, C.; Caballero, F. P.; Babonneau, F.; Gervais, C.; Laurent, G.; Titirici, M. M. Hydrothermal carbon from biomass: structural differences between hydrothermal and pyrolyzed carbons via ^{13}C Solid state NMR. *Langmuir* **2011**, *27*, 14460-

14471.

30 Baccile, N.; Laurent, G.; Babonneau, F.; Favon, F. Structure characterization of hydrothermal carbon spheres by advanced solid-state MAS ^{13}C NMR investigations. *J. Phys. Chem. C* **2009**, *113*, 9644-9654.

31 Baccile, N.; Falco, C.; Titirici, M. M. Characterization of biomass and its derived char using ^{13}C-solid state nuclear magnetic resonance, *Green Chem.* **2014**, *16*, 4839-4869.

32 Binder, J. B.; Gray, M. J.; White, J. F.; Zhang, Z. C.; Holladay, J. E. Reactions of lignin model compounds in ionic liquids. *Biomass Bioenergy* **2009**, *33*, 1122-1130.

33 Kawamoto, H.; Nakamura, T.; Saka, S. Pyrolytic cleavage mechanisms of lignin-ether linkages: a study on p-substituted dimers and trimers. *Holzforschung* **2008**, *62*, 50-56.

34 Samuel, R.; Foston, M.; Jaing, N.; Cao, S.; Ragauskas, A. J. HSQC (heteronuclear single quantum coherence) ^{13}C-^{1}H correlation spectra of whole biomass in perdeuterated pyridinium chloride–DMSO system: an effective tool for evaluating pretreatment. *Fuel* **2011**, *90*, 2836-2842.

35 Kim, H.; Ralph, J. Solution-state 2D NMR of ball-milled plant cell wall gels in DMSO-d6/pyridine-d5. *Org Chem Biomol Chem*. **2010**, *8*, 576-91.

36 Foston, M.; Nunnery, G. A.; Meng, X. Z.; Sun, Q. N.; Baker, F. S.; Ragauskas, A. J. NMR a critical tool to study the production of carbon fiber from lignin. *Carbon* **2013**, *52*, 65-73.

37 Ben, H. X.; Ragauskas, A. J. Heteronuclear Single-Quantum Correlation Nuclear Magnetic Resonance (HSQC-NMR) fingerprint analysis of pyrolysis oils. *Energy Fuels*. **2011**, *25*, 5791-5801.

38 Jiang, G.; Nowakowski, D. J.; Bridgwater, A. V. Effect of the Temperature on the Composition of Lignin Pyrolysis Products. *Energy Fuels.* **2010**, *24*, 4470-4475.

39 Greenwood, P. F.; van Heemst J. D. H.; Guthrie, E. A.; Hatcher, P. G. Laser micropyrolysis GC–MS of lignin. *J. Anal. Appl. Pyro.* **2002**, *62*, 365-373.

40 Pu, Y. Q.; Cao, S. L.; Ragauskas, A. J. Application of quantitative ^{31}P NMR in biomass lignin and biofuel precursors characterization. *Energy Environ. Sci.* **2011**, *4*, 3154-3166.

41 Ben, H. X.; Ragauskas, A. J. NMR Characterization of pyrolysis oils from kraft lignin. *Energy Fuels*. **2011**, *25*, 2322-2332.

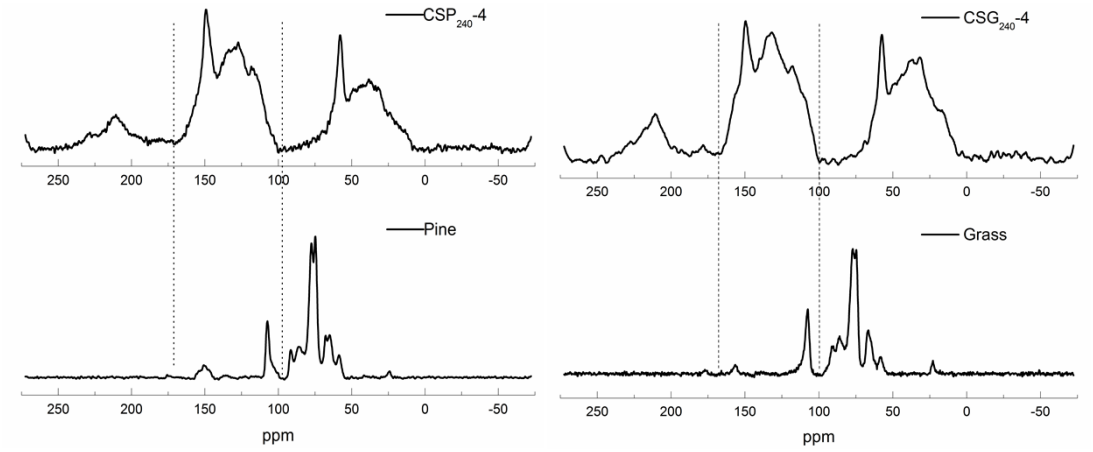

Fig.1 CP/MAS ^{13}C NMR spectra of LP, SG, CSP_{240}-4 and CSG_{240}-4.

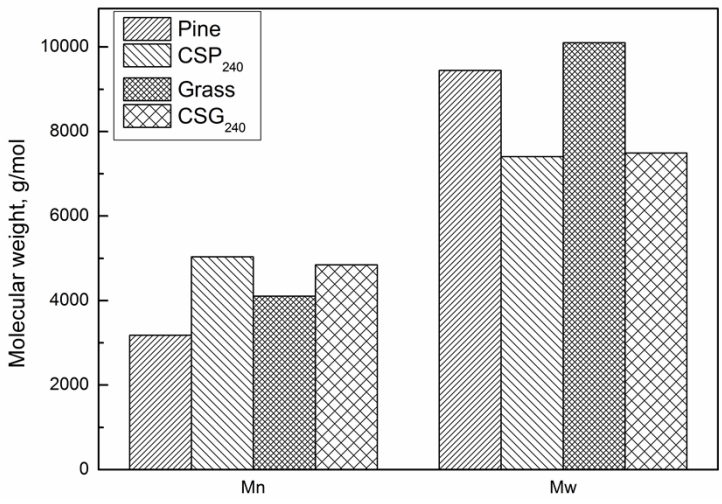

Fig. 2 Molecular weight distribution and PDI of LP, SG, CSP_{240}-4 and CSG_{240}-4.

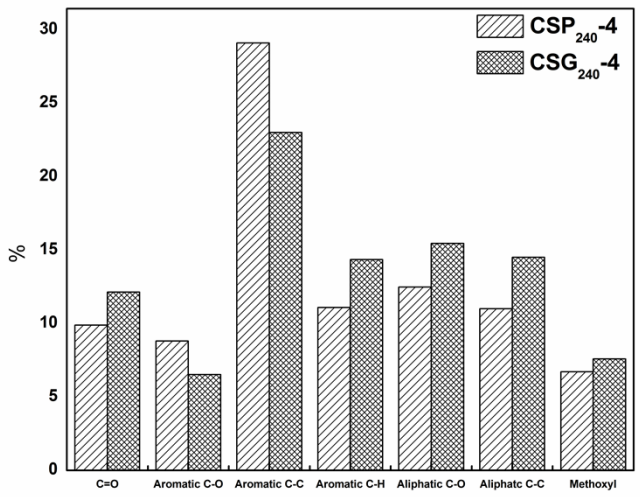

Fig. 3 Integration results for liquid products from CSP_{240}-4 and CSG_{240}-4, detected by

quantitative ^{13}C NMR, shown as the percentage of carbon.

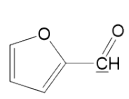

A

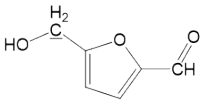

B

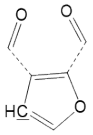

C

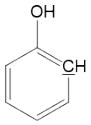

D

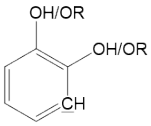

E

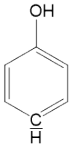

F

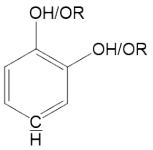

G

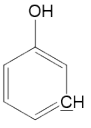

H

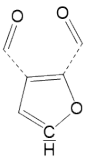

I

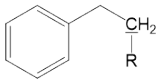

J

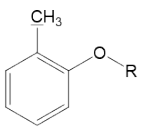

K

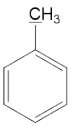

L

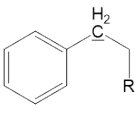

M

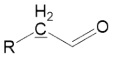

N

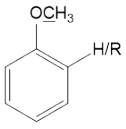

O_1

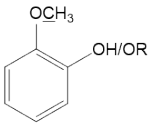

O_2

Fig. 4 Detailed structures of assignments for HSQC-NMR analysis [25-30].

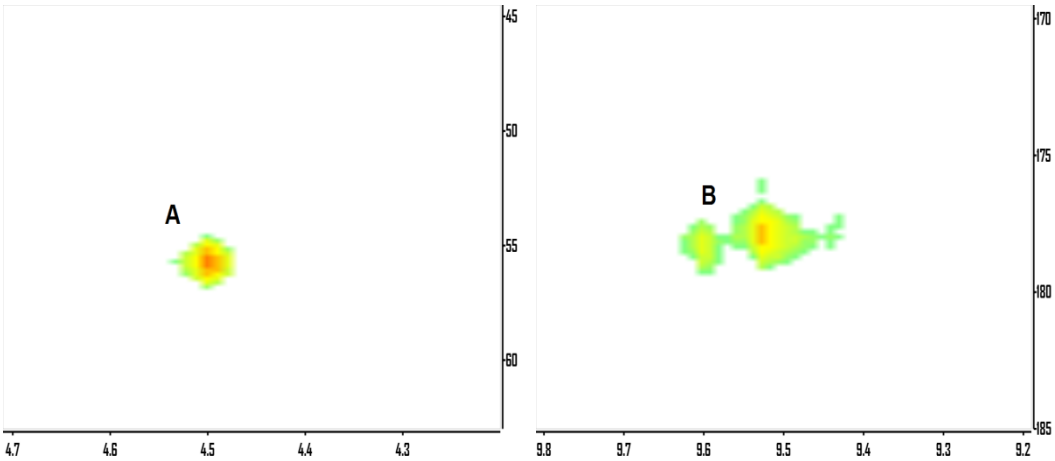

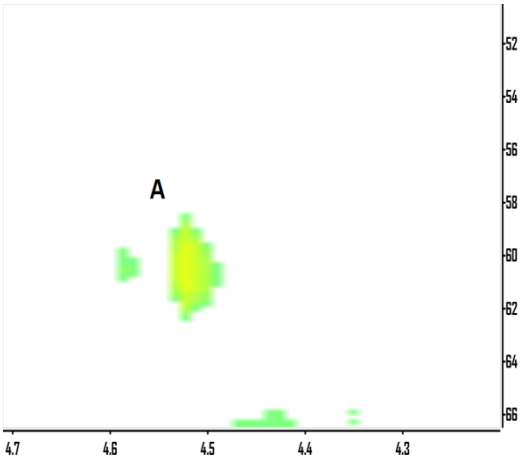

Fig. 5 HSQC-NMR assignment of HMF in liquid products of CSG_{240}-4 (up) and CSP_{240}-4 (down).

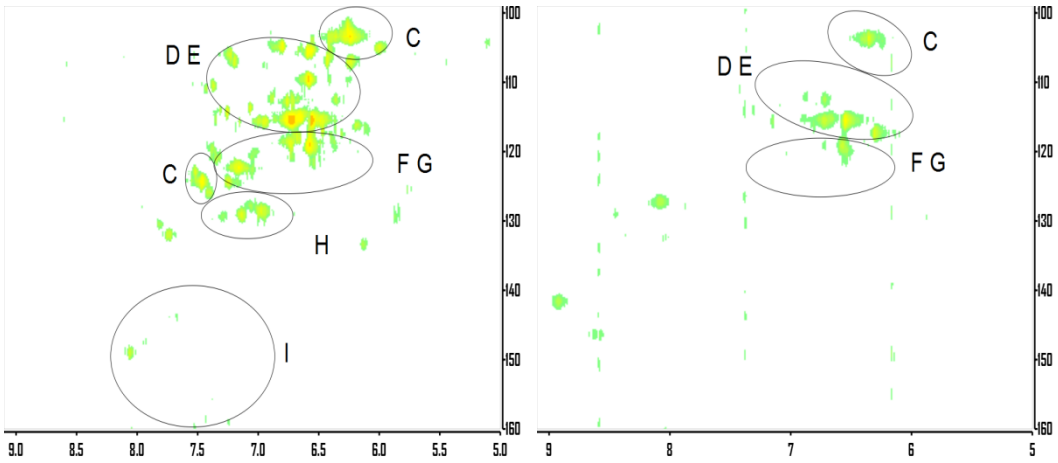

Fig. 6 HSQC-NMR assignment of Aromatic C-H bonds in liquid products of CSG_{240}-4 (left) and CSP_{240}-4 (right).

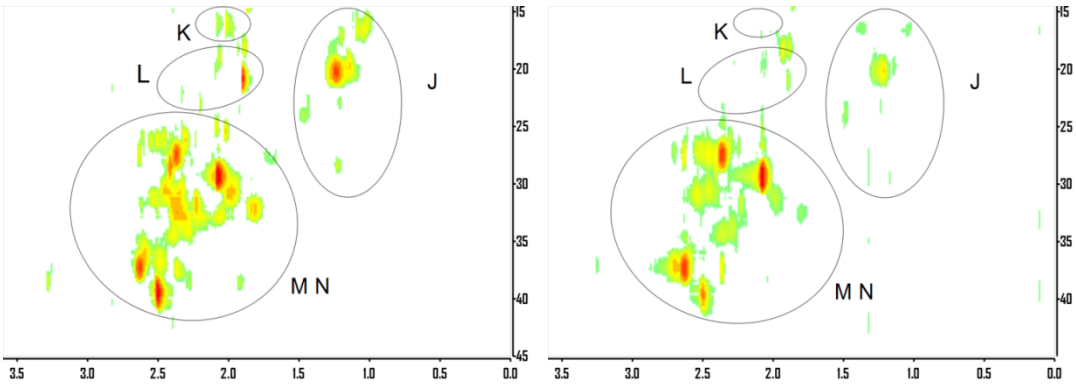

Fig. 7 HSQC-NMR assignment of Aliphatic C-H bonds in liquid products of CSG_{240}-

4 (left) and CSP_{240}-4 (right).

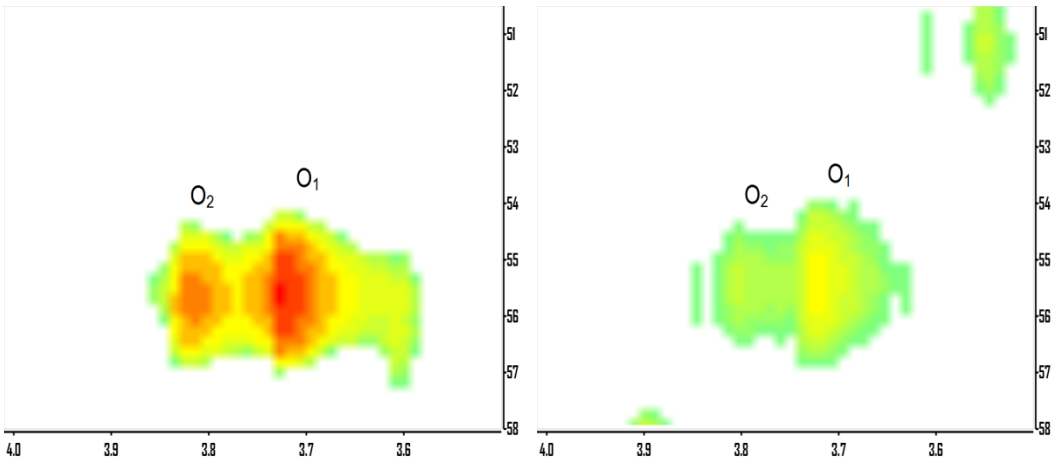

Fig. 8 HSQC-NMR assignment of methoxyl groups in liquid products of CSG_{240}-4 (left) and CSP_{240}-4 (right).

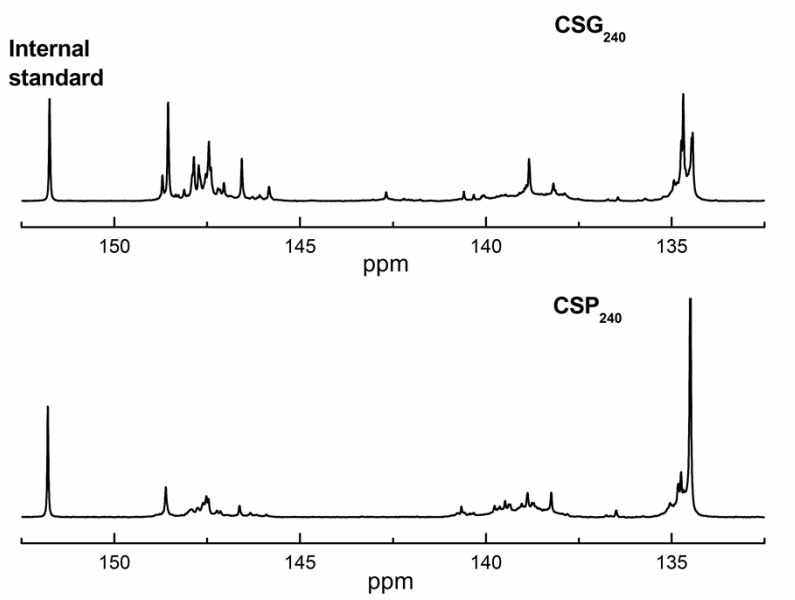

Fig.9 Quantitative ^{31}P NMR spectrum of CSP_{240}-4 and CSG_{240}-4 derivatized with TMDP using as NHND as internal standard.

Table 1 Chemical property of LP, SG, CSP_{240}-4 and CSG_{240}-4

Sample	Klason Lignin (%)	Yield (%)	Fixed Carbon Content (%)*	Ash (%)	HHV (MJ/kg)
LP	32.06	--	11.05	1.34	20.16
CSP_{240}-4	97.52	45.50	53.16	0.08	29.34
SG	24.91	--	14.77	1.97	16.23
CSG_{240}-4	94.67	41.93	48.61	0.42	23.94

*Fixed Carbon Yield (%) was calculated by thermogravimetry

Table 2 Hydroxyl groups contents of liquid products determined by quantitative ^{31}P NMR

Structure		Integration region [ppm]	CSP_{240}-4 mmol/g	CSG_{240}-4 mmol/g
Aliphatic OH (side-chain of lignin)		145.6-148.9	1.06	3.49
C_5 Substituted	β -5	142.3-142.9	--	0.09
Condensed	4-O-5	141.7-142.3	0.01	0.02
phenolic OH	5-5	140.1-141.2	0.26	0.06